Chaotic Photoconductivity

K. G. Kyritsi[1], L. Gallos[1], A. N. Anagnostopoulos[1], A. Cenys[2], and G. L. Bleris[3]

[1] *Physics Department, Aristotle University of Thessaloniki, GR-54006 Thessaloniki, GREECE*

[2] *Semiconductor Physics Institute, Gostauto 11, LT-2600 Vilnius, LITHUANIA*

[3] *Informatics Department, Aristotle University of Thessaloniki, GR-54006 Thessaloniki, GREECE*

(Received 10 October 1999)

In modern optoelectronics, light sensors are playing a main role. The present work examines the conditions of their performance, concerning photoconductivity. The model of a n-type photosensitive semiconductor containing two localized levels in its energy gap is considered. The semiconductor is illuminated homogeneously with bandgap-light and a constant electric field is applied. Electrons are excited by the illumination from the valence- to the conduction-band and by the electric field from the localized levels to the conduction-band. Electrons are also recombining from the conduction- to the valence-band and from the conduction-band to the localized levels. Depending on the parameters of the system (i.e. generation- and recombination rates, electric field strength, capture- and reemission-coefficients of the levels, ambient temperature, etc) the semiconductor is exhibiting periodic or chaotic conductivity. Different routes to chaos were observed in this system, like period doubling, intermittency and crisis induced intermittency.

Key words: chaos, period doubling, intermittency, photoconductivity

PACS numbers: 05.45, 72.40

1. Introduction

Currently much interest has been focused in nonlinear semiconductors with chaotic behavior [1]. In recent experiments on different kinds of crystals like *Ge* [2], [3], *GaAs* [4], etc. nonlinear phenomena such as period doubling , frequency locking, and chaotic oscillations have been discovered. Concerning nonlinear photoconductivity L.L.Golik et al. [5] have shown that a photoconductive n-type crystal with two localized levels in its energy gap shows chaotic behavior of the conductivity. In spite of the fact that the understanding of the physics of instabilities in semiconductors has been arrived at a satisfactory level, an explanation of the effects mentioned above becomes possible only now due to the advances of the chaos theory. Low-frequency photocurrent oscillations in *CdS* crystals occurring at constant applied voltage and illumination were described in [6]. This instability was also studied in other semiconductors [7], [8]. The explanation for this oscillatory behavior is based on the fact that a stable non-equilibrium state of the semiconductor becomes unstable because of temperature- or carrier concentration- fluctuations due to Joule heating [9]. L.L.Golik et al. in [10] reported also the observation of chaotic and complex periodic oscillations of photocurrent and temperature in photoconductive semiconductors. In the present paper we report a further investigation of the system proposed in [5] showing that under certain conditions also the period doubling and the crisis induced intermittency routes to chaos are possible.

2. The model

We consider a photosensitive n-type semiconductor with two levels located at E_1 and E_2 below its conduction band minimum E_c, with corresponding concentrations X_1 and X_2, Fig.1. It is supposed that the crystal is homogeneously illuminated with monochromatic light of constant intensity, corresponding to its energy gap E_g (i.e. $h\ nu = E_g$). After the stationary state is reached the generation rate G and the recombination rate R are constant and mutually equal.

In case the electric field $\mathcal{E}$ is applied on the crystal the electrons trapped in E_1 and E_2 are excited to the conduction band increasing the photocurrent rapidly and the sample temperature T rises due to inner Joule heating. This leads to depletion of the levels, recombination of free carriers and returning of the system to the initial state. This procedure can be repeated again and again leading to oscillations of the free carrier concentration n and of the temperature T. According to [5], [6] and [10] the system of differential equations (balance equations) governing the temporal changes of n and T and describing the photoconductor kinetics is the following one:

$$\frac{dn}{dt} = G - \frac{n}{\tau_r} - \sum_{i=1}^{2} \frac{dX_{ni}}{dt}, \quad (1)$$

$$\frac{dX_{ni}}{dt} = \gamma_i n(X_i - X_{ni}) - \gamma_i N_c X_{ni}; \quad i = 1,2; \quad (2)$$

$$\frac{dT}{dt} = Cn - \frac{1}{\tau_0}(T - T_0), \quad (3)$$

where the following symbols have been used: G is the generation rate; R is the recombination rate; n is the free electron concentration; p is the free hole concentration E_1, E_2 are two energy levels at E_1, E_2 below the conduction band E_C; X_1, X_2 are the concentrations of the levels E_1, E_2, respectively; X_{n1}, X_{n2} are the concentrations of electrons captured in the levels E_1, E_2; γ_1, γ_2 are the effective capture cross-sections of E_1, E_2, respectively; $\gamma_1 N_C$ and $\gamma_2 N_C$ are the effective emission cross-sections of E_1, E_2, respectively; τ is the free electron lifetime; $h\nu$ is the incident photon energy; $E_g = E_C - E_V$ is the energy gap; T is the sample temperature; $C = \frac{e\mu\mathcal{E}^2}{\rho C_V}$; e is the electron charge, μ is the electron mobility, ρ is the density, C_V is the specific heat, $\mathcal{E}$ is the applied electric field; T_0 is the ambient temperature; τ_0 is the characteristic cooling time of the sample.

3. The normalized system

To solve the previous system (1-3) numerically we transform it to following normalized and dimensionless one:

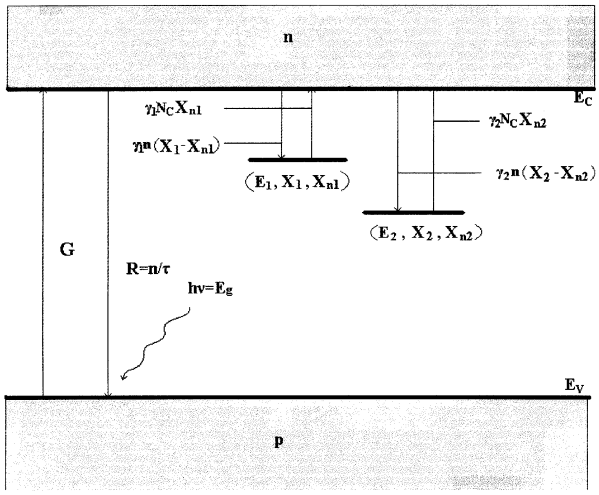

FIG. 1. The energy model of the considered n-type semiconductor including the two localized levels $E1$, E_2 in its energy gap.

$$\varepsilon_1 \frac{d\overline{n}}{d\tau} = 1 - \overline{n} + \sum_{i=1}^{2} \varepsilon_{2i} \left\{ \frac{\overline{X}_{ni}}{1+\beta_i} \right.$$
$$\left. \exp\left[\alpha_i \varepsilon_T \left(1 - \frac{1}{\overline{T}}\right)\right] - \overline{n}\left(1 - \frac{\beta_i}{1+\beta_i}\overline{X}_{ni}\right)\right\}; \quad (4)$$

$$\varepsilon_{3i} \frac{d\overline{X}_{ni}}{d\tau} = \overline{n}\left(1 + \beta_i - \beta_i \overline{X}_{ni}\right)$$
$$-\overline{X}_{ni} \exp\left[\alpha_i \varepsilon_T \left(1 - \frac{1}{\overline{T}}\right)\right]; \quad i = 1,2; \quad (5)$$

$$\varepsilon_4 \frac{d\overline{T}}{d\tau} = \overline{n}\,(1 - \varepsilon_T) - \overline{T} + \varepsilon_T. \quad (6)$$

If n_S, X_{niS}, T_S are the steady state solutions of the system (1a-1c) then the following substitutions have been used for the transformation of the system (1 - 3) to the system (4 - 6):

$$\tau = \frac{t}{\tau_{B1}(T_S)} \quad (7)$$

$$\overline{n} = \frac{n}{n_S}, \quad (8)$$

$$\overline{X}_{ni} = \frac{X_{ni}}{X_{niS}}, \quad (9)$$

$$\overline{T} = \frac{T}{T_S}. \quad (10)$$

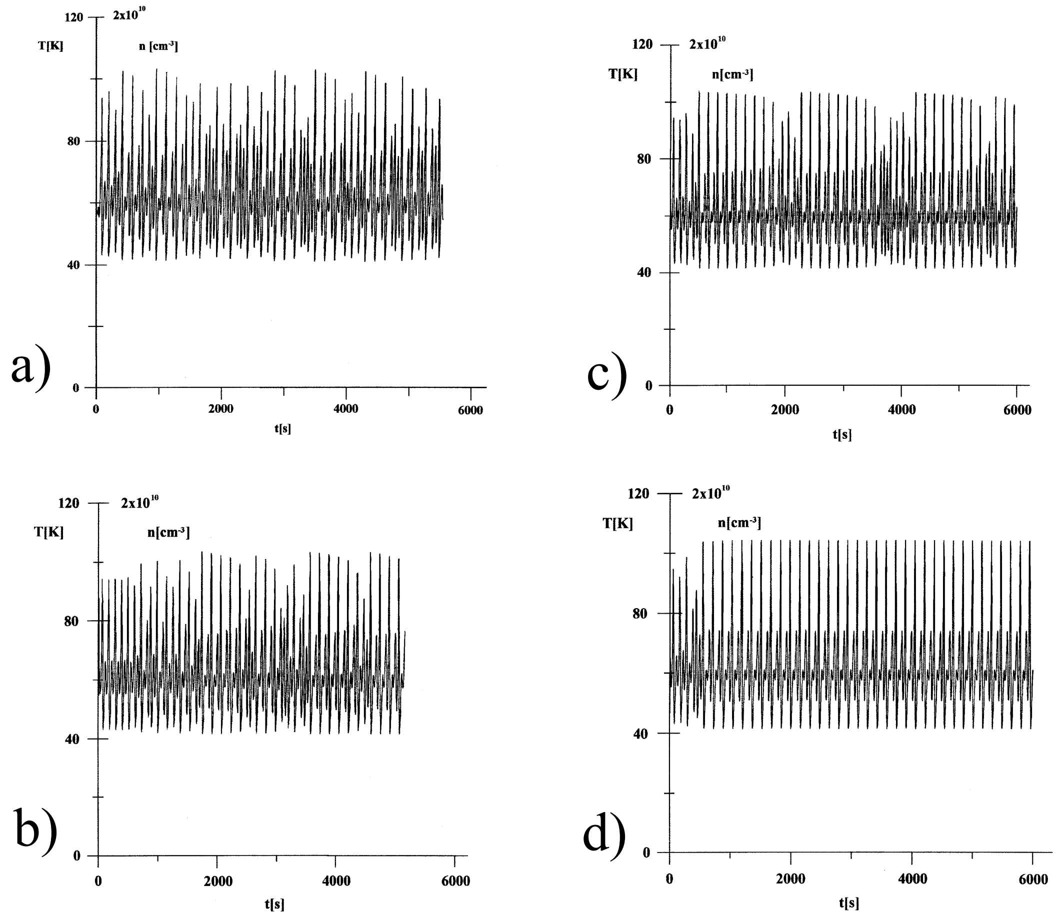

FIG. 2. Timeseries obtained for $5510K < E_1/k < 5525K$. a) Chaotic timeserie obtained for $E_1/k = 5517K$ b) Intermittent timeserie obtained for $E_1/k = 5521K$. Note that the periodic laminar lengths alternate with chaotic bursts. c) Intermittent timeserie obtained for $E_1/k = 5522.5K$. Note that as E_1/k increases the laminar lengths become longer and more frequent. d) Periodic timeserie obtained for $E_1/k = 5525K$.

Here

$$\tau_{B1} = \frac{1}{\gamma_i N_C},$$
$$n_S = G\tau_r,$$
$$X_{niS} = n_S X_i \left[n_S + N_C(T_S)\right]$$

for the temperature dependence of the free electron lifetime we have assumed in agreement with [5] and [11] that it is of the form

$$\tau_r(T) = \tau_{r0}\left[\exp\left(\frac{T - 380K}{25K}\right) = 1\right] \qquad (11)$$

the factors $\epsilon_1, \epsilon_{2i}, \epsilon_{3i}, \epsilon_4$ and ϵ_T characterizing the capture and reemission of electrons are given by the following relations:

$$\epsilon_1 = \frac{\tau_r}{\tau_{B1}(T_S)};$$
$$\epsilon_{2i} = \frac{\tau_r}{\tau_{ti}};$$
$$\epsilon_{3i} = \frac{\tau_{Bi}(T_S)}{\tau_{B1}(T_S)};$$
$$\epsilon_4 = \frac{\tau_0}{\tau_{B1}(T_S)};$$
$$\epsilon_T = \frac{T_0}{T_S} \qquad (12)$$

and the factors α_i, β_i and τ_{ti} used in the normalization are given by the following relations:

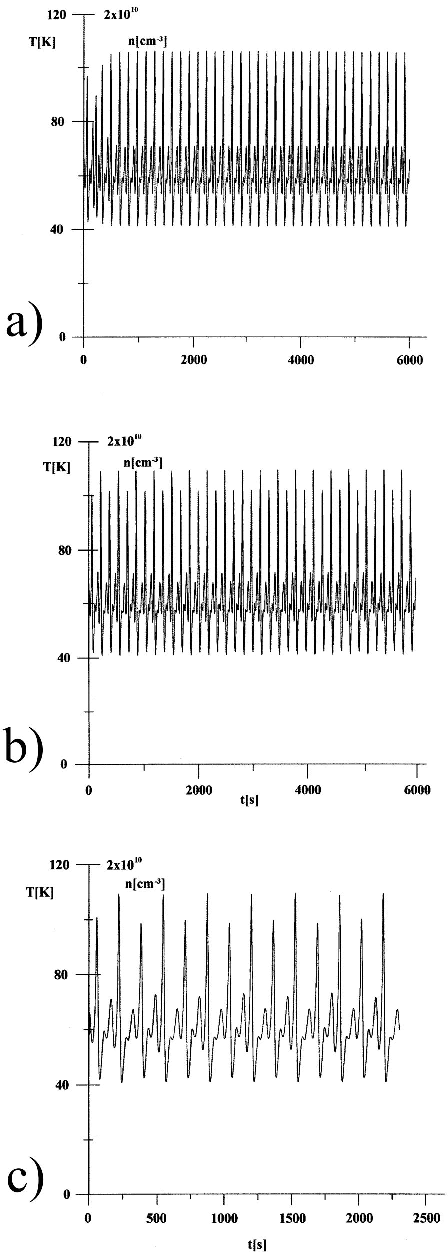

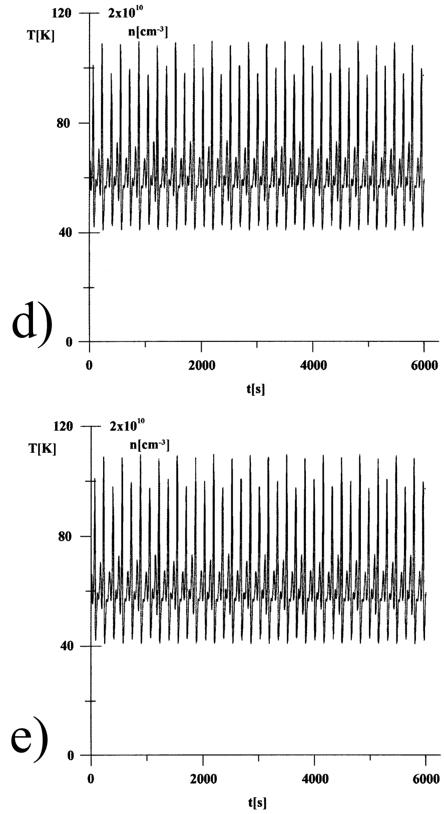

FIG.3 Timeseries obtained for $5550K < E_1/k < 5588K$. a) Periodic timeserie obtained for $E_1/k = 5550K$. Note the similarity of this timeserie with those of Fig. 2d. b) Periodic timeserie obtained for $E_1/k = 5580K$. Note that two frequencies are now present in the signal. c) Periodic timeserie obtained for $E_1/k = 5586K$. Note that four frequencies are now present in the signal. d) Periodic timeserie obtained for $E_1/k = 5587K$. Note that eight frequencies are now present in the signal. e) Almost chaotic timeserie obtained for $E_1/k = 5587.5K$.

$$\alpha_i = \frac{E_{ti}}{kT_0};$$

$$\beta_i = \epsilon_{2i}\left[\frac{G\tau_{Bi}(T_S)}{X_{ni}}\right];$$

$$\tau_{ti} = \frac{1}{\gamma_i X_{ni}};$$

$$\tau_{Bi}(T) = \frac{1}{\gamma_i N_C}.$$

4. Numerical solution and results

To solve the system (4 - 6) numerically the following values of the parameters have been used: $X_1 = 8.0\ 10^{15} cm^-3$; $5325K < \frac{E_1}{k} < 5949K$; $\gamma_1 = 1.79\ 10^{-13} cm^3/s$; $C = 0.2J/gK$; $X_2 = 3.5\ 10^{14} cm^{-3}$; $\frac{E_2}{k} = 6000K$; $\gamma_2 = 7.14\ 10^{-12} cm^3/s$; $\rho = 5.0 g/cm^3$; $T_0 = 283K$; $G = 2.0\ 10^{13} cm^{-3}s^{-1}$; $\mu = 10^2 cm^2/Vs$; $N_C = 2\ 10^{18} cm^{-3}$; $\tau_{r0} = 4.5\ 10^{-4}s$; $\mathcal{E} = 12000V/cm$; $\tau_0 = 3sec$.

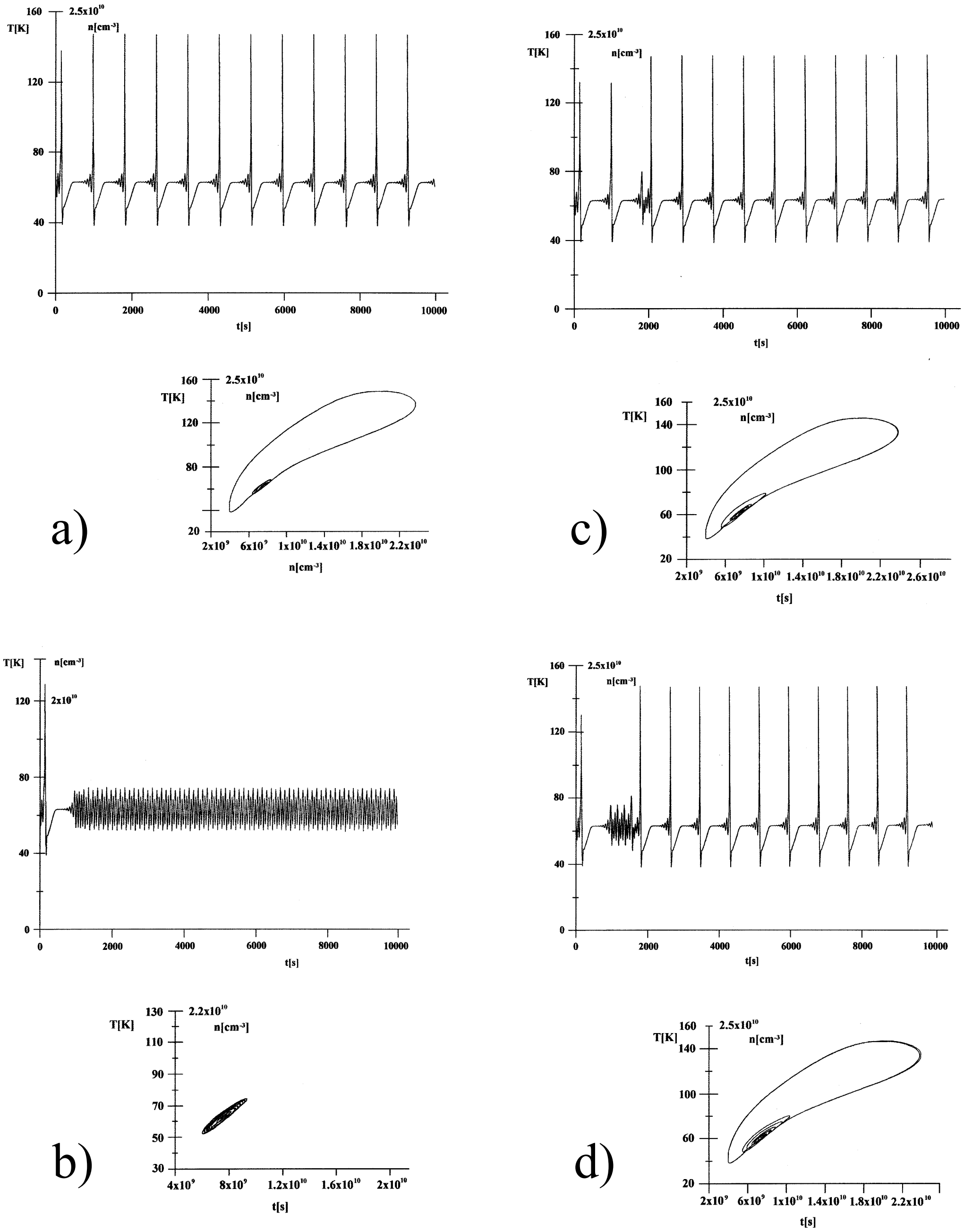

FIG.4. Timeseries obtained for $5948K < E_1/k < 5949K$. a) Timeserie obtained for $E_1/k = 5948K$. In the insert the large attractor dominating in the corresponding phase portrait is shown. b) Timeserie obtained for $E_1/k = 5949K$. In the insert the smaller attractor dominating in the corresponding phase portrait is shown. c) Timeserie obtained for $E_1/k = 5948.85K$. Note that the timeserie is almost similar to that of Fig.4a, except that a small part of the timeserie of Fig.4b is included in the present one. In the insert the attractor consist of two subattractors corresponding to the two previous ones of Figs. 4a, 4b. d) Timeserie obtained for $E_1/k = 5948.9278K$. Note that the timeserie is almost similar to that of Fig.4a, except that a larger part of the timeserie of Fig.4b is included in the present one. In the insert the attractor consist of two subattractors corresponding to the two previous ones of Figs. 4a, 4b.

These values correspond to data from [5], [12] and [13]. The numerical solution of the system (4 - 6) succeeded using a modified version of the well-known Runge-Kutta integration algorithm [14]. Both periodic and chaotic solutions were obtained (in the form of time series). Depending on the value of the position of E_1 , which served as the control parameter of the dynamical system the following routes to chaos were observed:

1. Intermittency of the I type, as E_1/k is shifted from 5322 K to 5325 K.
2. Period Doubling, as E_1/k moves from 5560 K to 5588 K.
3. Crisis induced Intermittency, as E_1/k changes from 5948 K to 5949 K.

1 The Intermittency route to chaos

For E_1/k values up to 5517 K the system has chaotic solutions, Fig. 2a. As E_1/k increases, this chaotic behaviour is interrupted by periodic laminar lengths, which become longer and more frequent, Figs 2b, 2c. Finally, for values higher than 5523 K the timeserie becomes almost periodic, Fig. 2d. This behaviour is typical for the intermittency route to chaos [15].

2 The Period Doubling route to chaos

The second route to chaos observed for E_1/k shifting from 5550 K to 5588 K is this of period doubling. For $E_1/k = 5550K$ the timeserie is a periodic one, Fig.3a, similar to that of Fig. 2d. As E_1/k increases the first period doubling is observed at 5580 K, Fig. 3b, the second one at 5586 K, Fig. 3c, the third one at 5587 K, Fig.3d and finally the orbit becomes chaotic at 5587.5 K, Fig.3e.

3 The Crisis Induced Intermittency

The third route to chaos was observed for E_1/k shifting from 5948 K to 5949 K. For E_1/k values up to 5948 K the timeserie has the form shown in Fig.4a. As E_1/k increases slightly to 5949 K the timeserie changes suddenly becoming entirely different both in shape and amplitude, Fig.4b. For E_1/k values between 5948 K and 5949 K the corresponding timeseries consist intermittently of parts of the two timeseries obtained for 5948 K and 5949 K, Figs. 4c-4e. From the corresponding phase portraits, (displayed as inserts in Figs. 4a-4e) it is obvious that at $E_1/k = 5948K$ only a large periodic attractor exists, which as E_1/k shifts from 5948 K to 5949 K, coexists with a second smaller one. Finally at $E_1/k = 5949$ K the first large attractor disappears and only the smaller one remains. This means that the basins of attractions of the two attractors (of the larger one for values of E_1/k lower than 5948 K and of the smaller one for values of E_1/k higher than 5949 K) as E_1/k is shifting from 5948 K to 5949 K are colliding, creating thus a behaviour described in [16] - [18] as an interior crisis. The corresponding intermediate forms of the timeserie are described as crisis induced intermittency [16].

5. Discussion

In ref.[5] the applied electric field served as the control parameter of the system (1 - 3) and only a period doubling route to chaos was observed. On the contrary in the present report the position of the shallower localized level E_1, was chosen as the control parameter, a fact that leads to the observation of three different routes to chaos as E_1 shifts in the energy gap, between E_C and E_2.

Acknowledgments

The authors acknowledge financial support from the EU (IC15-CT98-0820) and PENED 94. They also wish to thank Dipl. students I. Tanos, S. Stergianas and G. Katsikogiorgos for help in the calculations.

References

[1] H.L. Swinney. Physica D. **7**, 3 (1983)

[2] S.W. Teitsworth, R.M. Westervelt, and E.E. Haller. Phys. Rev. Letters. **51**, 825 (1983)

[3] G.A. Held, C.D. Jeffries, and E.E. Haller. Phys. Rev. Letters. **52**, 1037 (1984)

[4] E. Aoki, and K. Yamamoto. Phys. Letters A. **98**, 72 (1983)

[5] L. L. Golik, M.M. Gutman, and V. E. Pakseev. Phys. Stat. Sol. (b). **162**, 199 (1990)

[6] V.L. Vinetskii, I.D. Konozenko, and S.I. Shakhovtsova. Fiz. Tverd. Tela. **5**, 2698 (1963)

[7] S.G. Kalashnikov, V.I. Pustovoit, G.S. Pado, and E.F. Tokarev. Phys. Stat. Sol. **34**, 451 (1969)

[8] Y. Seki, S. Endo, and T. Irie. Japan. J. Appl. Phys. **19**, 1667 (1980)

[9] V.L. Vinetskii, S.I. Shakhovtsova, and I.D. Konozenko. Phys. Stat. Sol. **42**, 95 (1970)

[10] L.L. Golik, V.E. Pakseev, M.I. Elinson, and V.K. Yakushin. Fiz. Tekh. Poluprov. **20**, 2084 (1986)

[11] Yu.I. Balkarei, Yu.A. Rzhanov, L.L. Golik, and M.I. Elinson. Fiz. Tekh. Poluprov. **16**, 1558 (1982)

[12] R.H. Bube. J. Appl. Phys. **37**, 21 (1966)

[13] J. Woods, and K.N. Nicholas. Brit. J. Appl. Phys. bf 15, 1361 (1964)

[14] Numerical Recipes in C. W.H. Press, B.P. Flannery, S.A. Teukolsky, and W. Vetterling. Cambridge: "Cambridge University Press" Publishing. 1990. P. 569-580

[15] Deterministic Chaos. H.G. Schuster. Darmstadt Germany: "VCH Verlag" Publishing. 1989. P.98

[16] E. Ott. In: "Chaos in Dynamical Systems". Cambridge: "Cambridge University Press" Publishing. 1993

[17] C. Grebogi, E. Ott, and J.A. Yorke. Phys. Rev. Lett. **48**, 1507 (1982)

[18] C. Grebogi, E. Ott, and J.A. Yorke. Physica D. **7**, 181 (1983)